

# Molecular Motion of Polyethylene Chain-End Radicals Tethered on the Surface of Poly(tetrafluoroethylene) *in Vacuo* at Extremely Low Temperatures

Masato Sakaguchi\*

Ichimura Gakuen College, 61, Uchikubo,  
Inuyama 484, Japan

Shigetaka Shimada, Yasurō Hori, and  
Akihito Suzuki

Nagoya Institute of Technology, Gokiso, Nagoya 466, Japan

Fumio Kawaizumi

Department of Chemical Engineering, Nagoya University,  
Furo-cho, Nagoya 466, Japan

Masahiro Sakai and Shunji Bandow

Instrument Center, Institute for Molecular Science,  
Myodaiji, Okazaki 444, Japan

Received November 15, 1994

Revised Manuscript Received September 7, 1995

Numerous studies on the molecular motion of polyethylene (PE) chains in the bulk have been reported in which the molecular motion is frozen below its glass transition temperature. A glass transition temperature is dependent on the amount of free space around the chain. Usually in the bulk, a PE chain is surrounded by other PE chains and then has a limited space that reflects the glass transition temperature of 249 K.<sup>1</sup> Even if a PE chain has an intrinsically high mobility, this high mobility will be restricted in the bulk. If one PE chain has a large free space around its chain, this chain will be mobile far below 249 K.

We produced PE chains tethered on the surface of poly(tetrafluoroethylene) (PTFE) *in vacuo*. The PE chains have free radicals at the opposite terminals to the tethered points. These radicals are called "PE chain-end radicals" in this report. The molecular motion of PE chain-end radicals is measured by an electron spin resonance spectrometer (ESR). Here we report that PE chain-end radicals have three modes of molecular motion: (1) an overall rotation of the PE chain end at 2.8 K, (2) an exchange motion between two conformations of  $H_\alpha$  over 7 K, and (3) an oscillation of  $H_\beta$  over 30 K. All these characteristic temperatures are far below the glass transition temperature of PE. The high mobility of the PE chain-end radicals tethered on the PTFE surface *in vacuo* is probably due to a large free space around the chains.

**Experimental Section.** PTFE powder (Aflon G80, Asahi Glass Co., Ltd.) was used without further purification. Ethylene monomer (Takachiho Co., Ltd.) was purified by a freeze-pump-thaw method.

PE chain-end radicals tethered on the PTFE surface *in vacuo* are produced as follows: PTFE powder (1.5 g) is fractured with ethylene monomer (ca. 100 mL at 150 Torr at 307 K) *in vacuo* at 77 K for 21 h by a homemade vibration glass ball-mill.<sup>2</sup> During the milling, a mechanical fracture of PTFE produces PTFE mechano radicals,<sup>2</sup> which are chain end type radicals and are trapped on the fresh PTFE fresh surface produced by the fracture.<sup>3</sup> When the PTFE mechano radicals contact with ethylene monomer by a physical mixing during the milling, the PTFE mechano radicals initiate a radical polymerization of ethylene at 77 K.<sup>4</sup> This radical polymerization proceeds during the milling. Then propagating radicals of PE, i.e., PE chain-end radicals,

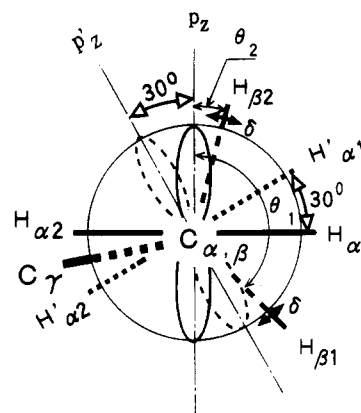


**Figure 1.** Two conformations of the PE chain-end radical. One conformation set with  $H_\alpha$  and  $p_z$  converts to another conformation depicted with  $H'_\alpha$  and  $p'_z$  by a 30° jump around the  $C_\alpha-C_\beta$  bond axis. The  $H_{\alpha 1}-C_\alpha-H_{\alpha 2}$  angle is put at 120°, in which the angle of  $C_\alpha-H_{\alpha 1}$  or  $C_\alpha-H_{\alpha 2}$  to the  $C_\alpha-C_\beta$  bond axis is assumed as +60 or -60° and holds during the jump motion.  $\theta$  is the dihedral angle of the  $C_\alpha-H_\beta$  bond axis relative to the  $p_z$  axis.  $\delta$  is an oscillation amplitude of  $H_{\beta 1}$  and  $H_{\beta 2}$ .

are obtained. Thus PE chain-end radicals are tethered on the PTFE surface *in vacuo*.

After the milling, the sample was dropped into an ESR sample tube at 77 K that was connected to the glass ball-mill.

An ESR spectrometer (Bruker ESP 300E) equipped with a helium cryostat (Oxford ESR 900) with a Au (0.07% Fe) vs chromel thermocouple was used to investigate the molecular motion of the PE chain-end radicals at extremely low temperatures. ESR spectra were observed at X-band frequency, at a microwave power level of 2  $\mu$ W to avoid power saturation, and with 100 kHz field modulation. The sample was cooled to 2.8 K in the cryostat and left to stand for 1 h; then the ESR spectrum was observed at 2.8 K. At elevated temperatures, the sample was kept for 15 min at each temperature and then observed at the temperature.

The specific surface area of the milled sample was obtained by the BET method<sup>5</sup> using a Micromeritics Flow Sorb II 2300 (Shimadzu Co.).

**Spectral Simulation.** Hori et al. have reported<sup>6</sup> a computer program based on a conformation exchange due to ring inversion of the cyclohexyl and cycloheptyl radicals in the respective thiourea complexes, in which each radical has one  $\alpha$  proton ( $H_\alpha$ ). This program employs the line shape equation derived by Heinzer<sup>7</sup> based on a density matrix theory in the Liouville representation. Heinzer's equation is, as expected, identical with that derived from the modified Bloch equations. The program assumes an exchange motion between two conformations which have an equal fractional population. It is also assumed that a rate constant of a transition from one conformation to the other is independent of the direction for the transition.

We have modified the computer program developed by Hori et al. to simulate and ESR spectrum of a primary alkyl radical which has two  $H_\alpha$ 's with an anisotropic hyperfine splitting and two  $\beta$  protons ( $H_\beta$ ) with an isotropic hyperfine splitting. The intramolecular coordinates based on the principal axes of the hyperfine splitting tensor of  $H_\alpha$  are assumed:  $A_x$  is parallel to  $P_z$  occupied by the unpaired electron at the  $\alpha$  carbon ( $C_\alpha$ ), the  $A_z$  axis is along the direction of the  $C_\alpha-H_{\alpha 1}$  bond axis, and the  $A_y$  axis is perpendicular to both the  $A_x$  and  $A_z$  axes. It is assumed that  $H_{\alpha 1}$  and

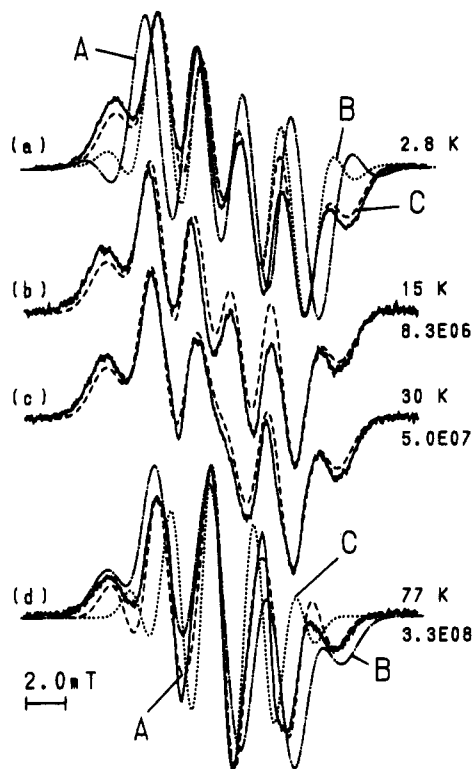


**Figure 2.** (a) Observed and simulated spectra of PE chain-end radicals. (—): observed at 2.8 K. Curve A (— · —): simulated by an anisotropic hyperfine splitting of  $H_\alpha$  and an isotropic hyperfine splitting of  $H_\beta$  based on  $A_{\text{iso}} = 2.30$  mT and  $\rho_c B_2 = 5.00$  mT assuming a frozen exchange motion and oscillation. Curve B (···): simulated as in curve A except  $A_{\text{iso}} = 2.07$  and  $\rho_c B_2 = 4.14$  mT. Curve C (---): simulated as in curve B except for axial symmetric hyperfine splitting with  $A_\perp = 1.62$  mT and  $A_\parallel = 2.96$  mT. (b) (—): observed at 15 K. (---): simulated as in curve C in (a) except the exchange rate is  $8.3 \times 10^6$  s $^{-1}$ . (c) (—): observed at 30 K. (---): simulated as in curve C in (a) except the exchange rate is  $5.0 \times 10^6$  s $^{-1}$  and the oscillation amplitude is 7°. (d) (—): observed at 77 K. Curve A (— · —): simulated as in curve C in (a) except the exchange rate is  $3.3 \times 10^8$  s $^{-1}$  and the oscillation amplitude is 11°. Curve B (···): simulated as in curve A except the frozen oscillation. Curve C (···): simulated by assuming free rotation of  $H_\alpha$  based on the identical  $A_{\text{iso}}$  and  $\rho_c B_2$  with curve A.

$H_{\alpha 2}$  are put at symmetrical positions to the  $C_\alpha$ – $C_\beta$  bond axis with angles of +60 and –60°. A dihedral angle between two  $H_\beta$ 's is assumed as 120°.

Another molecular coordinate system of axial symmetry due to a rotation of the chain is assumed: the  $A_\parallel$  axis is parallel to a rotational axis, and the  $A_\perp$  axis is perpendicular to  $A_\parallel$ .

Figure 1 shows two conformations of the PE chain-end radical.

**Results and Discussion.** *Identification of the PE Chain-End Radical.* The ESR spectrum of the milled sample was observed at 2.8 K (solid line in Figure 2a). The simulated spectrum (curve A, dash-dot line in Figure 2a) is calculated from the anisotropic hyperfine splitting of  $H_\alpha$  with angles of +60 and –60° to the  $C_\alpha$ – $C_\beta$  bond axis ( $A_x = 2.2$  mT,  $A_y = 3.5$  mT, and  $A_z = 1.2$  mT $^8$ ), and the isotropic hyperfine splittings of  $H_{\beta 1}$  and  $H_{\beta 2}$  ( $A_{\beta 1}(\theta_1=135^\circ) = 2.50$  mT and  $A_{\beta 2}(\theta_2=15^\circ) = 4.67$  mT). These hyperfine splittings are based on an isotropic term ( $A_{\text{iso}} = 2.30$  mT) of the anisotropic hyperfine splitting and  $\rho_c B_2$  (5.00 mT) $^8$  in primary alkyl radicals, where  $B_2$  is the empirical parameter used in the McConnell equation $^9$  and  $\rho_c$  is the spin density at  $C_\alpha$ . The anisotropic hyperfine splitting means that any

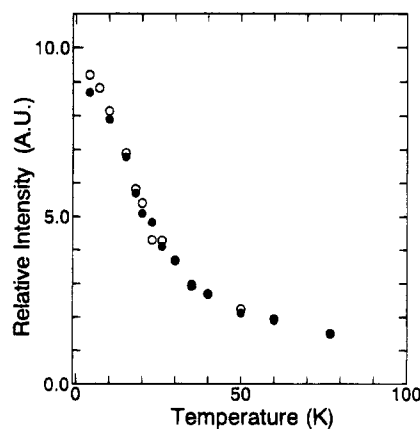


**Figure 3.** Concentrations of PE chain-end radicals with increasing temperature (O) and decreasing temperature (●).

motion of  $H_\alpha$  is frozen. Curve A is too wide and thus is a very poor fit to the observed spectrum. Another simulated spectrum (curve B, dotted line in Figure 2a) is calculated from the anisotropic hyperfine splitting of  $H_\alpha$  with angles of +60 and –60° ( $A_x = 2.00$  mT,  $A_y = 3.20$  mT, and  $A_z = 1.00$  mT) and the isotropic hyperfine splittings of  $H_{\beta 1}$  and  $H_{\beta 2}$  ( $A_{\beta 1}(\theta_1=135^\circ) = 2.07$  mT and  $A_{\beta 2}(\theta_2=15^\circ) = 3.86$  mT). These hyperfine splittings are based on  $A_{\text{iso}}$  (2.07 mT) and  $\rho_c B_2$  (4.14 mT). Curve B is improved but is still a poor fit to the observed spectrum at the outer part of the spectrum. The simulated spectrum (curve C, broken line in Figure 2a) is obtained by using values of  $A_{\beta 1}$ ,  $A_{\beta 2}$ , and  $A_{\text{iso}}$  identical with those of curve B except an axial symmetric hyperfine splitting of  $A_\perp(H_\alpha) = 1.62$  mT and  $A_\parallel(H_\alpha) = 2.96$  mT. Curve C is in good agreement with the observed spectrum. Thus the observed spectrum is assigned to  $-\text{CH}_2\text{CH}_2^\bullet$ , that is, PE chain-end radicals. Furthermore, the axial symmetric hyperfine splitting suggests an overall rotation of the radicals. Thus, overall rotation of PE chains probably occurs even at 2.8 K.

Initially, we made various trials using typical values of  $A_{\text{iso}}$  and  $\rho_c B_2$  in primary alkyl radicals to simulate the ESR spectrum observed at 2.8 K. However, we failed to get an appropriate simulation spectrum. For example, the simulated spectrum with typical values of a primary alkyl radical of  $A_{\text{iso}}$  (2.30 mT) and  $\rho_c B_2$  (5.0 mT) $^8$  gave a very poor fit (curve A in Figure 2a) or also a poor fit (not shown) even with no allowance for dihedral angle between two  $H_\beta$ 's with less than 100°. In contrast, the best fit simulation spectrum (curve C in Figure 2a) is obtained with  $A_{\text{iso}} = 2.07$  mT and  $\rho_c B_2 = 4.14$  mT. However, these  $A_{\text{iso}}$  and  $\rho_c B_2$  values are too small compared to the typical values,  $A_{\text{iso}} = 2.25$ – $2.30$  mT and  $\rho_c B_2 = 5.0$ – $5.38$  mT. $^{8,10,11}$  Generally, these values are dependent on  $\rho_c$ , which is affected by the substituent on the radical and the matrix surrounding the radical. In our case, PE chain-end radicals are tethered on the PTFE surface which is composed of fluorine atoms with a large electron affinity (3.399 eV). $^{12}$  Thus, those small values seem to be due to the low spin density at  $C_\alpha$ , which may cause leaking to the fluorine atoms comprising the PTFE surface.

*Exchange Motion of  $H_\alpha$ .* The ESR spectra of PE chain-end radicals were observed at 15, 30, and 77 K (solid lines in Figure 2b,d). Spectral changes beginning at 7 K (not shown) are clearly evident in the center region of the spectrum at 15 K and continue with increasing temperature to 77 K. This spectral change was reversible in the temperature range 2.8–77 K. No change of

**Table 1. Proton Hyperfine Splitting Constants and Oscillation Amplitudes Determined by Simulation**

temp (K)	hyperfine splitting (mT)			exchange rates (s <sup>-1</sup> )	hyperfine splitting (mT)			oscillation (⟨δ <sup>2</sup> ⟩ <sup>1/2</sup> (deg))
	A <sub>⊥</sub>	A <sub>∥</sub>	A <sub>iso</sub>		A <sub>β1</sub> (θ <sub>1</sub> )	A <sub>β2</sub> (θ <sub>2</sub> )	A <sub>β</sub> av	
2.8	1.62	2.96	2.07	exc rigid	2.07	3.86	2.96	0
7	1.62	2.96	2.07	1.4 × 10 <sup>6</sup>	2.07	3.86	2.96	0
15	1.62	2.96	2.07	8.3 × 10 <sup>6</sup>	2.07	3.86	2.96	0
30	1.62	2.96	2.07	5.0 × 10 <sup>7</sup>	2.05	3.83	2.94	7
77	1.74	2.72	2.07	3.3 × 10 <sup>8</sup>	2.33	3.48	2.90	11

radical concentration was observed at the same temperature on the increasing process and on the decreasing process (Figure 3). These results indicate that the spectral change is attributed to a temperature dependence of a molecular motion of the radicals.

The simulated spectrum of 7 K (not shown) was obtained by using A<sub>⊥</sub> = 1.62 mT, A<sub>∥</sub> = 2.96 mT, A<sub>β1</sub> = 2.07 mT, and A<sub>β2</sub> = 2.96 mT and an exchange motion of H<sub>α</sub> (Figure 1) with a rate of 1.4 × 10<sup>6</sup> s<sup>-1</sup> (Table 1). The 15 K simulated spectrum (broken line in Figure 2b) was obtained by using hyperfine splittings identical with those of the 7 K simulated spectrum and an exchange rate of 8.3 × 10<sup>6</sup> s<sup>-1</sup>. The 15 K simulated spectrum is in good agreement with the observed spectrum. Thus the exchange motion occurs over 7 K and more clearly at 15 K.

As shown in Table 1, A<sub>⊥</sub> increases over 30 K but A<sub>∥</sub> decreases; however, A<sub>iso</sub> is independent of temperature. This constant A<sub>iso</sub> indicates that the spin density of H<sub>α</sub> is not affected by temperature. Thus this fact is additional evidence that the spectral change is attributed to the molecular motion.

**Oscillation of H<sub>β</sub>.** A<sub>β</sub> has a temperature dependency over 30 K (Table 1). A<sub>β2</sub> and an average (A<sub>βav</sub>) of A<sub>β1</sub> and A<sub>β2</sub> decrease but A<sub>β1</sub> increases with increasing temperature. These A<sub>β</sub>'s are determined by the best fit simulation spectra (curve C in Figure 2a, broken lines in b, c and curve A in d).

Hori et al. have reported<sup>6</sup> a temperature dependence of A<sub>β</sub> as follows: The magnitude of A<sub>β</sub> is calculated from the following well-known McConnell equation:<sup>9</sup>

$$A_{\beta} = B_0 + \rho_c B_2 \cos^2(\theta + \delta) \quad (1)$$

where θ is the dihedral angle of the C<sub>β</sub>-H<sub>β</sub> bond axis relative to the p<sub>z</sub> axis at the equilibrium state and δ is the amplitude of an oscillation of H<sub>β</sub>. B<sub>0</sub> and B<sub>2</sub> are empirical parameters. B<sub>0</sub> is neglected in the following discussion. Under the condition of an identical ⟨δ<sup>2</sup>⟩ for each H<sub>β</sub>, the following two equations are given:

$$A_{\beta 1} = 1/2 \rho_c B_2 \{1 + \cos 2\theta_1 (1 - 2 \langle \delta^2 \rangle)\} \quad (2)$$

$$A_{\beta 2} = 1/2 \rho_c B_2 \{1 + \cos 2\theta_2 (1 - 2 \langle \delta^2 \rangle)\} \quad (3)$$

A<sub>βav</sub> is given by eqs 2 and 3 when considering the oscillation

$$A_{\beta av} = 1/2 (A_{\beta 1} + A_{\beta 2}) = 1/2 \rho_c B_2 \{1 + 1/2 \cos(2\theta_1 - \pi/3) - \langle \delta^2 \rangle \cos(2\theta_1 - \pi/3)\} \quad (4)$$

where a dihedral angle of 120° between two H<sub>β</sub>'s is

assumed. This equation indicates that the A<sub>βav</sub> approaches 1/2 ρ<sub>c</sub> B<sub>2</sub> from 1/2 ρ<sub>c</sub> B<sub>2</sub> {1 + 1/2 cos(2θ<sub>1</sub> - π/3)} with increasing temperature under the oscillation.

We estimated an oscillation amplitude, (⟨δ<sup>2</sup>⟩)<sup>1/2</sup>, by using eq 4 with ρ<sub>c</sub> B<sub>2</sub> = 4.14 mT, θ<sub>1</sub> = 135°, θ<sub>2</sub> = 15°, and A<sub>β</sub> determined by a best fit simulation spectrum. The (⟨δ<sup>2</sup>⟩)<sup>1/2</sup> is shown in Table 1. Below 30 K, oscillation does not take place in the molecular motion. However, over 30 K, the amplitude of the oscillation increases with increasing temperature.

When the oscillation is neglected, the simulated spectrum (curve B in Figure 2d) is a poor fit to the observed spectrum.

Another simulated spectrum (curve C in Figure 2d) was calculated by an isotropic hyperfine splitting A<sub>iso</sub> (2.07 mT) and an identical hyperfine splitting A<sub>β1</sub> = A<sub>β2</sub> (2.07 mT), in which free rotation of H<sub>α</sub> around the C<sub>α</sub>-C<sub>β</sub> bond axis is assumed. This simulated spectrum is a very poor fit to the observed spectrum. This poor fit indicates that H<sub>α</sub> does not freely rotate around the C<sub>α</sub>-C<sub>β</sub> bond axis at 77 K.

We conclude that overall rotation of the PE chain-end radicals probably occurs even at 2.8 K. Furthermore, the exchange motion of H<sub>α</sub> between two conformations takes place over 7 K, and in addition the oscillation of H<sub>β</sub> occurs over 30 K.

The area per tethered point on the PTFE surface (3.1 × 10<sup>3</sup> Å<sup>2</sup>/point) was deduced from the radical concentration (6.8 × 10<sup>16</sup> spins/g) and the specific surface area (2.1 m<sup>2</sup>/g). This value of the area per tethered point suggests that there is a large free space around the PE chains tethered on the PTFE surface *in vacuo*.

We conclude that the high mobility of the PE chain-end radicals tethered on the PTFE surface *in vacuo* is due to a large free space around the PE chains.

## References and Notes

- (1) *Polymer Handbook*; Brandrup, J., Immergut, E. H., Eds.; John Wiley & Sons: New York, 1989; p IV-214.
- (2) Sakaguchi, M.; Sohma, J. *J. Polym. Sci., Polym. Phys. Ed.* **1975**, *13*, 1233.
- (3) Kurokawa, N.; Sakaguchi, M.; Sohma, J. *Polym. J.* **1978**, *10*, 93.
- (4) Sakaguchi, M.; Sohma, J. *J. Appl. Polym. Sci.* **1978**, *22*, 2915.
- (5) Brunauer, S.; Emmell, P. H.; Teller, E. *J. Am. Chem. Soc.* **1938**, *90*, 309.
- (6) Hori, Y.; Shimada, S.; Kashiwabara, H. *J. Phys. Chem.* **1986**, *90*, 3037.
- (7) Heinzer, J. *Mol. Phys.* **1971**, *22*, 167.
- (8) Kasai, P. H. *J. Am. Chem. Soc.* **1990**, *112*, 4313.
- (9) Heller, C.; McConnell, H. M. *J. Chem. Phys.* **1960**, *32*, 1535.
- (10) Adrian, F. J.; Cochran, E. L.; Bowers, V. A. *J. Chem. Phys.* **1973**, *59*, 3946.
- (11) Fessenden, R. W.; Schuler, R. *J. Phys. Chem.* **1963**, *39*, 2147.
- (12) *CRC Handbook of Chemistry and Physics*, 69th ed.; Weast, R. C., Ed.; CRC Press: Boca Raton, FL, 1988-1989; p E64.

MA9464130